1   Automated cryo-lamella preparation for high-throughput *in-situ*

2   structural biology

3   Authors:

4   Genevieve Buckley[1,2], Gediminas Gervinskas[3], Cyntia Taveneau[1,2], Hari Venugopal[3], James C.

5   Whisstock[1,2,4,5], Alex de Marco[1,2,4,*]

6   1 ARC Centre of Excellence in Advanced Molecular Imaging, Monash University

7   2 Biomedicine Discovery Institute, Department of Biochemistry and Molecular Biology, Monash

8   University, Clayton Australia

9   3 Clive and Vera Ramaciotti Centre for Cryo-Electron Microscopy, Monash University, Clayton

10   Australia

11   4 University of Warwick, Coventry CV4 7AL, United Kingdom

12   5 EMBL Australia, Monash University, Clayton Australia

13   * Correspondence to alex.demarco@monash.edu

14

15   Keywords:

16   Cryo-FIB, cryo-lamella, automation, cryo-EM, in situ structural biology

17   Abstract

18   Cryo-transmission electron tomography (cryo-ET) in association with cryo-focused ion beam (cryo-FIB)

19   milling enables structural biology studies to be performed directly within the cellular environment.

20   Cryo-preserved cells are milled and a lamella with a thickness of 200-300 nm provides an electron

21   transparent window suitable for cryo-ET imaging. Cryo-FIB milling is an effective method, but it is a

22   tedious and time-consuming process, which typically results in ~10 lamellae per day. Here, we

23   introduce an automated method to reproducibly prepare cryo-lamellae on a grid and reduce the

24   amount of human supervision. We tested the routine on cryo-preserved *Saccharomyces cerevisiae*

25   and demonstrate that this method allows an increased throughput, achieving a rate of 5 lamellae/hour

26   without the need to supervise the FIB milling. We demonstrate that the quality of the lamellae is

27   consistent throughout the preparation and their compatibility with cryo-ET analyses.

28

29 ## Introduction

30 Today, the best method to image the cellular environment in its native state and obtain structural

31 information is Cryo-Electron Tomography (cryo-ET) (Beck & Baumeister, 2016). Biological samples are

32 vitrified by fast freezing at cryogenic temperature (80 – 120 Kelvin) and then imaged using a cryo-

33 Transmission Electron Microscope (TEM) following a tomographic acquisition scheme. Cryogenic

34 fixation is instantaneous and it helps to reduce the effects of radiation damage during data acquisition

35 (Dubochet et al., 1988). This process ensures that all the water contained in the sample is vitreous,

36 therefore solid and capable of withstanding the high-vacuum environment of TEMs while not

37 diffracting the electron beam. As a general guideline, the maximum allowed sample thickness is

38 ~300nm, since most cryo-TEM operate at 300 keV where an electron statistically undergoes a single

39 elastic scattering event in ~250 nm of water (elastic mean free path) (Holtz, Yu, Gao, Abruña, & Muller,

40 2013). Thicker samples provide higher chances of inelastic scattering, which in non-crystalline samples

41 cannot be interpreted as useable information. Since cells are typically multiple microns thick, the

42 inspection is limited to the thinnest regions such as filopodia (Carlson et al., 2010; Stauffer et al., 2014;

43 Weber, Wojtynek, & Medalia, 2019). The first approach that made it possible to inspect the inside of

44 a cryo-preserved cell through cryo-ET was cryo-sectioning of vitreous sections (CEMOVIS) (Al-Amoudi

45 et al., 2004). CEMOVIS has the advantage of potentially allowing serial-section tomography with

46 minimal losses throughout the cell, but it is extremely difficult to perform and suffers from mechanical

47 deformations and is prone to surface contamination (Al-Amoudi, Studer, & Dubochet, 2005).

48 Alternatively, using an extremely common approach in semi-conductor sciences, it is possible to

49 isolate a thin lamella of material using a dual-beam microscope which utilizes a Scanning Electron

50 Microscope (SEM) for imaging and a Focussed Ion Beam (FIB) for machining any sample with

51 nanometre resolution (Marko, Hsieh, Schalek, Frank, & Mannella, 2007; Rigort et al., 2012; Schaffer

52 et al., 2015; Schaffer et al., 2017). Cryo-FIB milling has been shown to be a highly effective method for

53 preparing cellular sections for cryo-electron tomography (Rigort et al., 2012; Schaffer et al., 2015;

54 Schaffer et al., 2017; Villa, Schaffer, Plitzko, & Baumeister, 2013), but it is time-consuming since the

55 resolution and the milling speed are inversely proportional.

56 In contrast to industrial FIB applications (e.g. semi-conductors), all existing procedures for cryo-

57 lamellae preparation are performed manually due to the heterogeneity and dose-sensitivity of

58 biological specimens. The immediate effect is that highly trained users are performing an extremely

59 repetitive task. This not only results in an elevated cost, but it also restricts production to a throughput

60 of 5-10 lamellae per day (Danev, Yanagisawa, & Kikkawa, 2019; Koning, Koster, & Sharp, 2018; Wolff

61 et al., 2019). Further, in most cases, cryo-FIB microscopes are only used for one session/day while

62 users are onsite, therefore to boost the productivity night shifts are the only way forward. Cryo-ET

2

63 acquisition can already run unsupervised and regardless of the acquisition scheme used it is possible

64 to obtain at least 20 tomograms over 24 hours. Data collection schemes optimized for high resolution

65 will require ~60 min of acquisition time per tomogram (Hagen, Wan, & Briggs, 2017), while fast

66 tomography workflows will allow for acquisition times down to 5 minutes (Chreifi, Chen, Metskas,

67 Kaplan, & Jensen, 2019; Eisenstein, Danev, & Pilhofer, 2019). Moving beyond the bare throughput and

68 instrument usage, since FIB milling is a manual and iterative process the reproducibility scales with

69 the user experience. Recognising the need for reproducible sample preparation, several workflows

70 and best practice procedures have been developed (Hsieh, Schmelzer, Kishchenko, Wagenknecht, &

71 Marko, 2014; Medeiros et al., 2018; Schaffer et al., 2015), but the initial steep learning curve still

72 represent a limitation especially for laboratories where in house expertise has not yet been

73 established.

74 One way to counteract the low throughput of cryo-lamella preparation consists of targeting a region

75 based on the known presence of an interesting event or structure. In order to achieve this level of

76 efficiency, the typical approach uses correlative light and electron microscopy techniques which, when

77 properly performed, prevents from imaging areas that do not contain useful information for a specific

78 study (Arnold et al., 2016; Gorelick et al., 2019). Regardless of the correlative microscopy approach in

79 use, the mismatch between the throughput of cryo-ET and the preparation of lamellae is evident. Here

80 we introduce an automated and reproducible method for on-grid cryo-lamella preparation for vitrified

81 cell. We demonstrate an increased throughput capable of reproducibly producing ~5 lamellae/hour.

82 Since the presented protocol can run unsupervised, the learning phase for new users will be shorter

83 than the current situation. Further, with the appropriate cryo-stage, this protocol opens the possibility

84 for a 24/7 cryo-lamellae preparation.

Materials and methods

85

Cell culture and sample cryo-fixation

86

87 *Saccharomyces cerevisiae* was cultured in YPD at 30 degrees, cells were harvested when an optical

88 density of 0.6 was reached. Cells were washed twice in PBS and re-suspended in half of the initial

89 volume. 5 µL of cell-containing solution was deposited on a Cu-300 R2/2 grid (Quantifoil™) which had

90 been previously glow discharged for 30 seconds using a Pelco EasyGlow™. Excess solution was

91 removed through manual blotting and cells were vitrified by plunge freezing in a liquid 60/40

92 Ethane/propane mix and stored in liquid nitrogen.

Cryo-FIB milling

93

94 All tests presented here were conducted on a ThermoFisher Helios Ux G4 DualBeam™ equipped with

95 a Leica cryo-stage and a VCT500 cryo-transfer system. Grids were clipped in autogrid cartridges prior

96 to loading into the cryo-FIB.

97 Cryo-FIB control and scripting

98 All manual operations were conducted through the ThermoFisher Xt UI™, while batch cryo-FIB

99 operations were performed using Python 3.6 through the communication API ThermoFisher

100 Autoscript 4.1™ (which is required to control the microscope). Scientific python packages used include

101 numpy, scipy, matplotlib, scikit-image, click, pyyaml and pytest (Hunter, 2007; Oliphant, 2007; S. van

102 der Walt, Colbert, & Varoquaux, 2011; Stéfan van der Walt et al., 2014).All original scripts used in this

103 procedure are installable via the pip package installer for Python. All the source code and the

104 instructions   can   be   downloaded   from   the   laboratory   webpage

105 (www.github.com/DeMarcoLab/autolamella).

106 Cryo-TEM

107 Cryo-electron tomograms and micrographs were collected on a ThermoFisher Titan Krios G3 equipped

108 with a post-GIF Gatan K2™ DDE camera. Images were collected in EFTEM mode following a low-dose

109 acquisition scheme. The microscope setup included a 50 µm condenser aperture and a 70 µm

110 objective aperture. All tomograms were imaged from -60 to +60 deg with 3 deg increment. The total

111 dose on the tilt-series was 98.4 e$^-$/Å^2, with a dose-rate of 4e$^-$/pixel/sec and tilt micrographs were

112 collected at a nominal magnification of 42000x resulting in a final pixel-size of 3.61 Å. Low

113 magnification overviews were collected at a nominal magnification of 2500x in LM mode, resulting in

114 a final pixel-size of 20 nm.

115 Tomography reconstruction

116 Tilt-series were aligned using patch tracking and back-projected using Etomo from the IMOD suite

117 (Mastronarde, 1997). Tomogram visualization and filtering occurred through IMOD or UCSF Chimera

118 (Pettersen et al., 2004).

119 Image display and figure preparation

120 All figures have been prepared using Adobe Illustrator. Cropping, filtering and contrast adjustments

121 have been performed using IMOD or Fiji. Videos have been made using Fiji (Schindelin et al., 2012).

122

Results and discussion

124 Any TEM sample preparation procedure based on FIB milling requires the following operations:

125 changing the milling current and/or energy, changing the imaging parameters, stage movements for

126 sample realignment, beam-shift for drift compensation and setup/positioning of the milling patterns.

127 On average, every milling step can require time spanning from a few seconds to multiple minutes and

128 the sequence is extremely repetitive and predictable. In this situation, even the most diligent operator

129   will incur a significant time-waste as a consequence of short delays at the start of every step and due

130   to the time required to perform manual realignment.

131   Here, we analysed the preparation workflow and reduced its complexity to the 4 steps: (i)

132   identification of the regions of interest; (ii) opening the lamellae (trenching); (iii) thinning and (iv)

133   polishing the lamellae. Cryo-FIB milling occurs in a high-vacuum environment where the pressure

134   rages from 2e-6 to 5e-7 mBar. Under these conditions the atmosphere around the sample is not

135   completely depleted from water, therefore, the slow growth of a crystalline ice layer on the sample

136   surface is expected over time. Typical contaminations rates measured as crystalline water deposition

137   are specified by the instrument manufacturers to be in the order of 5 – 20 nm/hour. In addition, the

138   material that is sputtered while milling can redeposit on neighbouring areas, therefore contaminating

139   finished lamellae. To limit contamination, we concluded that the best course of action is to run the

140   lamella preparation protocol in 3 or more stages. Accordingly, we defined a default protocol that

141   includes 3 stages, first the routine loops through all the regions of interest and open the trenches,

142   then lamellae are thinned to ~500 nm and last they are polished to the desired thickness (100-300

143   nm). Following this protocol, the bulk material removal, which also represents the most time-

144   consuming part is carried out over the first two steps, while the polishing step is performed over the

145   last few minutes prior to unloading the sample. The default number of stages for the preparation of

146   the lamellae is three, but users can add or remove stages if the number of conditions required to

147   achieve good lamellae is different on other samples. The presented routine includes stage movement,

148   beam current changes and, most importantly, it requires time. Accordingly, there will be drift and

149   relocation errors to be accounted for. Our proposed protocol follows a low-dose approach similar to

150   the one performed in cryo-ET, where a sacrificial area containing a fiducial marker is used for tracking

151   and focussing, whereas the sample area is imaged only once at low-dose and magnification to define

152   the location of the region of interest.

153   Figure 1 shows a flowchart diagram of the program logic. We minimized the required user interaction:

154   the user provides a configuration file when launching the program (an example file is provided with

155   the package) which contains all the conditions required for the lamella preparation. The parameters

156   defined in the configuration file are fixed for each batch job and include the milling and imaging

157   currents, the depths, the field of view size, as well as the fiducial and the lamella sizes. The milling

158   depth for lamellae and fiducials are set in the configuration file, but, where required, they can be set

159   independently for each location. This decision was made to provide a good compromise between the

160   flexibility and setup time. Lamellae locations are interactively selected together with the location of

161   the tracking area. In order to improve reproducibility, a small cross-shaped fiducial marker is FIB milled

162   in the centre of the tracking area. The fiducial marker assists image re-alignment after stage

5

163   movements and shifts due to changes in the ion beam current. The image containing the fiducial
164   marker is updated after every re-alignment to take care of eventual degradations that might occur in
165   response to imaging. In principle, this area can be used to correct against drift during the milling
166   procedure, but we found that on two systems with different cryo-stages (both ThermoFisher Helios
167   G4) this option is not needed given the short time that each milling stage requires. Since the sample
168   thickness can vary substantially across locations, we kept the possibility to adjust the desired FIB
169   milling depth individually for each lamella and fiducial. This setup procedure is repeated for as many
170   locations as the user wishes to mill and the only constraint here is the time required for milling. The
171   user is guided step-by-step throughout the setup phase (for examples through the workflow see
172   supplementary figures 3-6). The tracking area is also used to re-align the lamella position when
173   compensating for the beam convergence (Schaffer et al., 2017). For this option, users are able to
174   define the amount of over/under-tilt to apply in relation to the current and instrument in use.

175   Since the tracking procedure follows a low-dose acquisition scheme, the site where the lamella will be
176   prepared is going to be imaged only once using the ion beam and twice using the SEM (optional). In
177   order to help the users during the protocol optimization for each sample and for documentation
178   purposes, we added the option to acquire full-field ion beam images at each stage of the process, but
179   in general, this option would not be used so the sample conditions can remain pristine. The ion beam
180   image that is acquired at the beginning of the process to define the lamella position and the tracking
181   area generally will have a low resolution and fast dwell time to minimize the dose applied to the
182   sample. In our experiments, we have found that a field of view of 50 µm acquired with a pixel size of
183   32nm provides a good image quality when using 10-30 pA of current with dwell times comprised
184   between 50 and 300 nsec. Under these conditions, the dose is extremely low but the alignment
185   precision is limited by the pixel size. Accordingly, we have set the possibility of acquiring the tracking
186   images (restricted to the sacrificial area) with a smaller pixel size (e.g. 8 or 16 nm) and dose, therefore
187   making the alignment process significantly more precise. Further, in order to increase the flexibility in
188   case a user needs to image samples that do not align efficiently with the provided algorithm, we set
189   up the code structure to allow custom frequency filtering and real space masks to be applied, or even
190   the replacement of the alignment function with another algorithm.

191   In figure 2 we show a gallery through the lamella preparation procedure. The cross mark visible in the
192   image represents the centre of the tracking area and has a size of 6×6 µm. In order to respond to the
193   variability of the sample topology, we made sure that the position of the fiducial and the lamella can
194   be selected and do not have a strict relative position. The only limits set are to prevent the milling
195   areas to overlap between fiducial and lamella as well as to prevent any of the two areas to be outside
196   the field of view.

6

197 We tested the robustness of the procedure by setting up batch preparation jobs with multiple (3-5)

198 lamellae. Our results indicate high reproducibility throughout each job with lamellae thicknesses

199 always comprised between 210 nm and 250 nm. The throughput was measured to be 4 to 5

200 lamellae/hour depending on the sample thickness. In supplementary figure 1, we show a gallery

201 comprising 5 lamellae which have been prepared in 47 minutes from the beginning of the batch

202 procedure. The setup phase (selecting sites and defining tracking markers) for that job required

203 approximately 12 minutes. In order to ensure that the quality of the samples is not compromised, we

204 inspected all lamellae through cryo-TEM (see figure 3 and supplementary figure 2), and imaged a

205 subset via cryo-ET (figure 4 and supplementary video), therefore ensuring the suitability for

206 downstream analyses. The level of curtaining is comparable to what has previously been reported

207 from manual preparation. Although in this case, we have noticed that the length of the lamella directly

208 correlates with the level of curtaining. This observation correlates with the fact that we applied the

209 same ion dose when preparing all lamellae (supplementary figure 2).

210 Our results show that by automating the lamella preparation it is possible to prepare uniform lamellae

211 with the desired thickness at a rate which is far greater than what could be reproducibly achieved with

212 manual operation. The average preparation time for 1 lamella is ~9 minutes, excluding sample loading,

213 initial alignment and selection of the regions of interest. From experience, users will require about 1

214 hour for stage cooling and sample loading, then Pt deposition and general imaging of the samples for

215 navigation will require ~10-15 min. Then, when the procedure starts, the basic navigation is conducted

216 through the microscope UI and the user must ensure that when a region of interest is selected the

217 sample is at the coincidence height. This is important because the overview images acquired with the

218 SEM before and at the end of the milling procedure can provide immediate feedback on the quality of

219 each lamella before going to the cryo-TEM. If the stage is not at the correct height the SEM images

220 will not include the lamella site. Further, if the user chooses to compensate for the beam convergence

221 (optional), the stage tilt will change by 1-4 deg. If the stage is not at the correct height the region of

222 interest will move outside the field of view. Our experience shows that the user supervised part of the

223 procedure which includes the selection of the regions of interest and the preparation of the fiducial

224 requires ~2-3 minutes/site. Accordingly, if a user loads 2 grids and selects 20 sites/grid the preparation

225 time from stage cooling to the completion of 40 lamellae would be between 10 and 11 h, with the

226 polishing step conducted through the last 1.5 h.

227 The typical duration of a cryo-FIB session is limited by the liquid nitrogen supply (ThermoFisher and

228 Quorum cryo-stages can be kept cold for ~11 h, while Leica cryo-stages have the possibility to refill

229 the liquid nitrogen dewar and provide sessions that are longer than 24 h). The automation and the

230 fact that the procedure runs mostly unsupervised ensures that for ~8 h users do not need to be on-

231 site. Accordingly, this opens up the possibility to prepare cryo-lamellae with a 24 h continuous

232 operation of the microscope and therefore lead to ~80 or more lamellae/day. Considering the latest

233 developments in regards to fast cryo-ET acquisition it will be possible to match this throughput on the

234 TEM (Chreifi et al., 2019). Even in the situation where the above-described throughput is not required,

235 a protocol providing up to 40 lamellae during a daytime session will shorten the user queue around

236 cryo-FIBs, therefore, allowing more projects to be conducted in facilities where the availability of

237 instrumentation is limited in relation to the number of users.

238

239

240 Acknowledgements

247

248   Figures
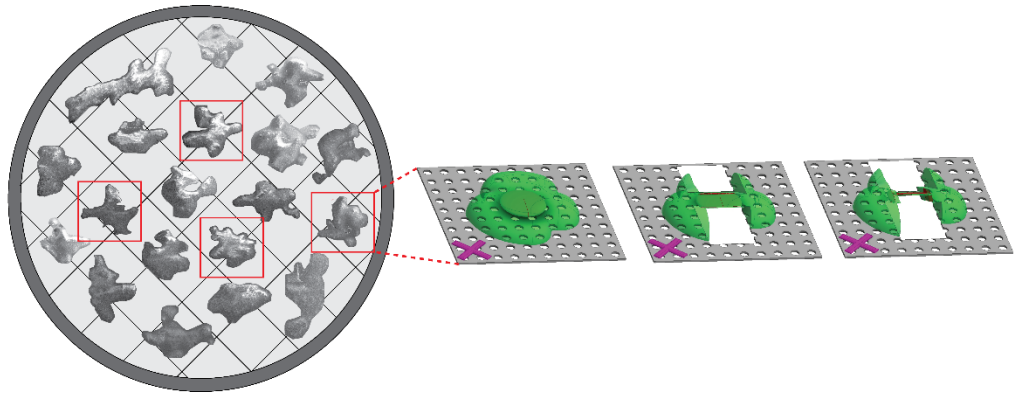
249

250   **Graphical abstract.**

9

251
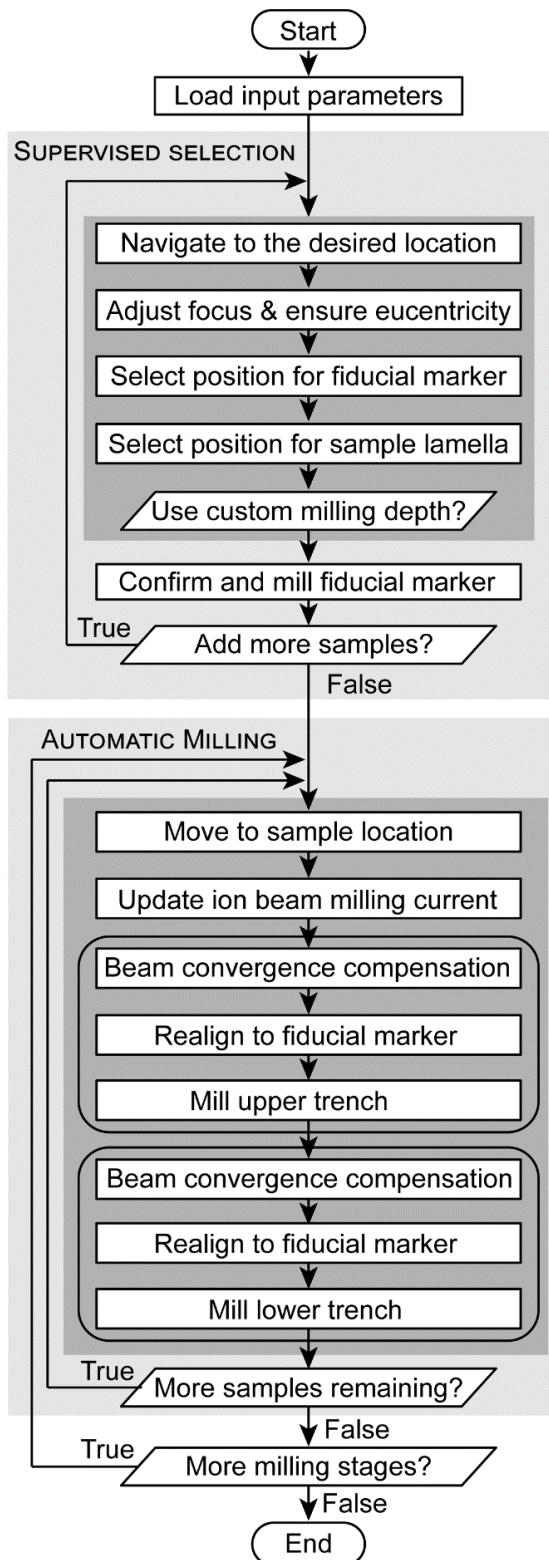
Figure 1: Flowchart of the automated cryo-lamella process. First, a configuration file containing all the required parameters is loaded (e.g. lamella size, currents, etc.). The process can be divided into two sections, a human supervised section followed by the automated lamella preparation across all selected locations. The supervised section requires users to interactively select the locations. The general navigation can be performed through the ThermoFisher Xt UI™ or ThermoFisher MAPS™

257   (where available). In order to achieve an optimal performance, the user must adjust the focus and

258   ensure the sample stage is at the coincidence point between the FIB and SEM beams. The position of

259   the fiducial marker (used for image realignment) and the lamella can be defined anywhere within the

260   field of view. This section is performed as many times as the number of lamellae required. Once all

261   sites of interest have been selected the automated section starts. Here, automated ion beam milling

262   is performed for all selected samples. First, the initial trenches are opened for every sample (typically

263   using a higher milling current). Then the FIB milling current is reduced and every sample is further

264   thinned until the final polishing step. Every time the sample stage is moved or the FIB milling current

265   is changed, the sample position is checked using the fiducial marker and correction is done through

266   beam-shift. The compensation for the beam convergence can be specified in the input configuration

267   file and can be changed for each milling stage.

268

269
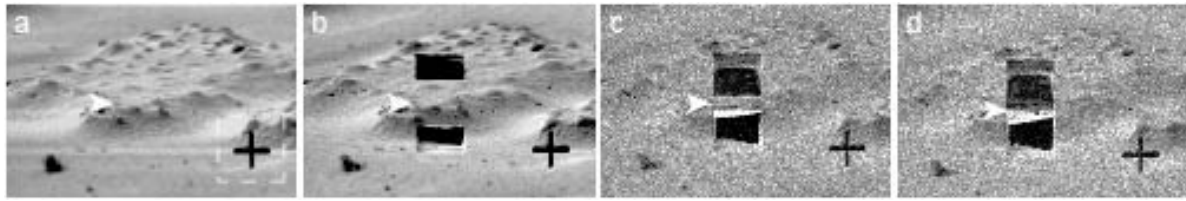
Figure 2: Ion beam images of a single lamella during the automated FIB milling. (a) A cross-shaped fiducial marker is created for later image realignment, reduced area field of view used for realignment shown by dashed white box; (b) trenches are milled above and below the lamella using a current of 2.4 nA; (c) the lamella is thinned further using an intermediate ion beam current, 75 pA; (d) the completed lamella after final ion beam milling at low current, 26 pA. White arrowheads indicate the position of the finished lamella; the scale is indicated by 6×6 μm cross-shaped fiducial marker.

278
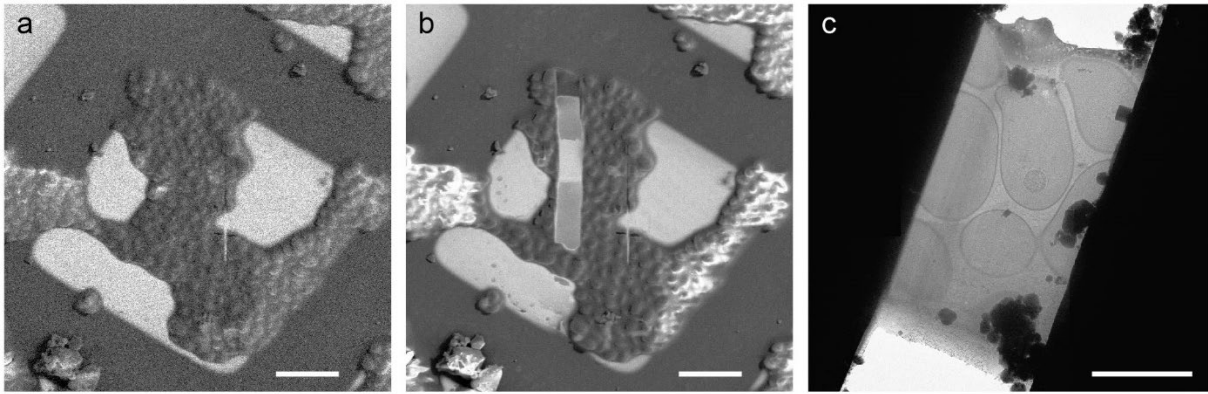
279 **Figure 3: View of an exemplary lamella from cryo-SEM and low magnification cryo-TEM.** (a) shows a

280 cryo-SEM view of a region before the lamella preparation; (b) shows the same region after sample

281 preparation. Both SEM images have been acquired as part of the automated procedure. (c) shows a

282 low magnification cryo-TEM overview of the same lamella displayed in a and b. The surface quality is

283 comparable to what has previously been reported from manual preparation. Scale-bars in (a) and (b)

284 are 20 μm, while in (c) the scale bar 5 μm.

285

286

13

287
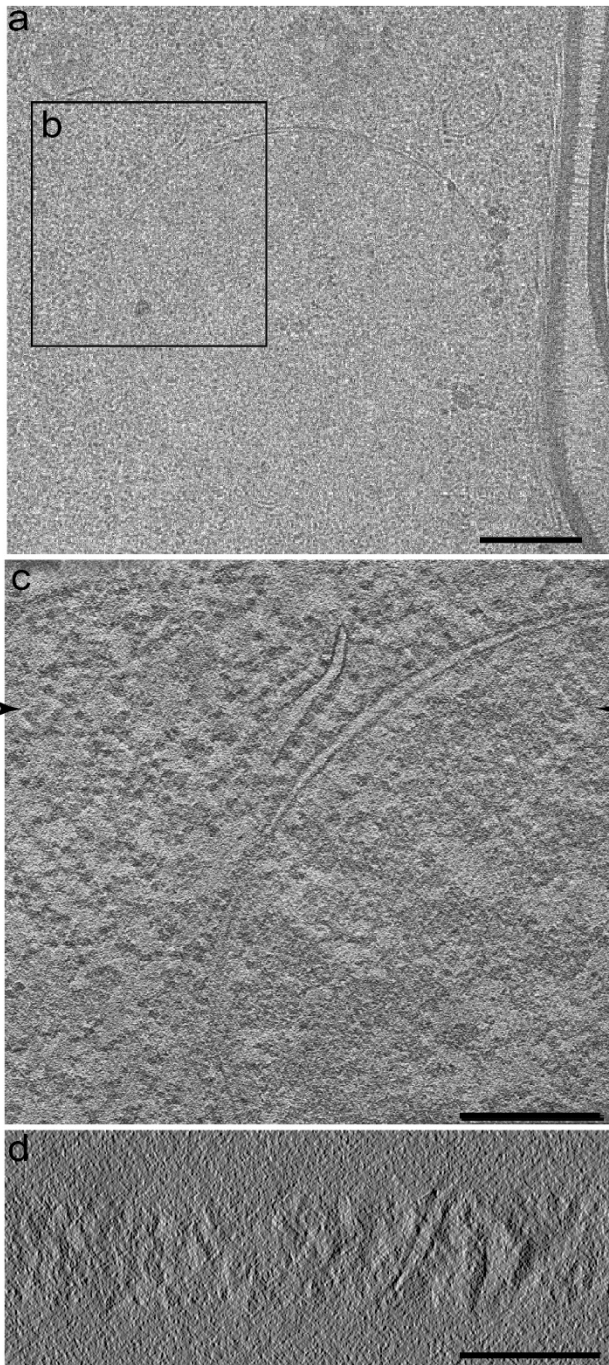
Figure 4: Cryo-TEM and cryo-ET performed on the same lamella shown in figure 2. Panel (a) shows a mid-magnification (6500x) micrograph of the lamella. Inset (b) in panel (a) corresponds to the XY slice from the tomogram collected and displayed in (c). Panel (d) shows a XZ slice through the tomogram. The arrowheads in (c) show the position of the slice in displayed in (d). Scale-bars are 500 nm in (a) and 200 nm in (c) and (d).

293

14

294   Supplementary Information
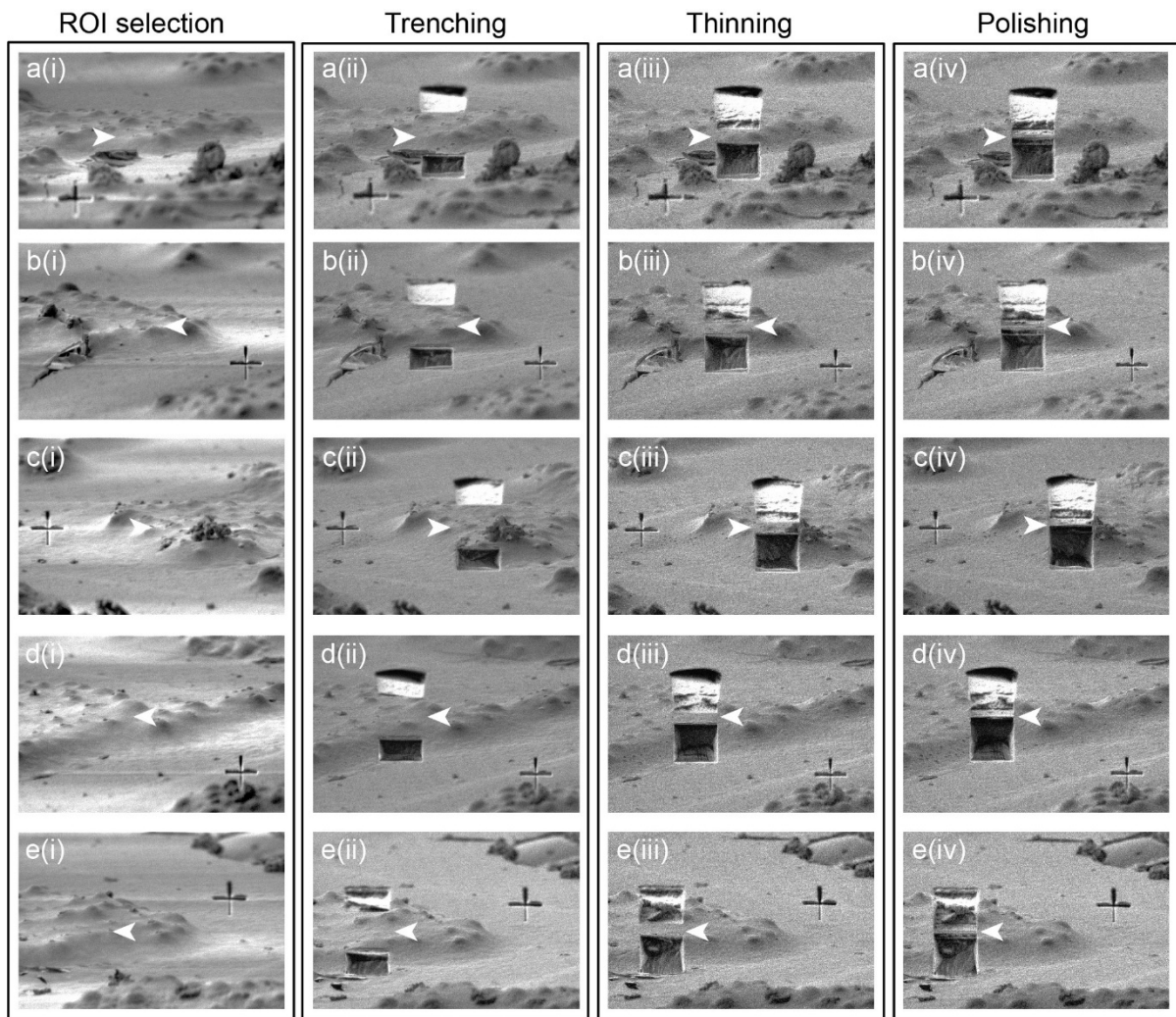
295

296   **Supplementary figure 1: Ion beam images acquired throughout a single batch job consisting of 5**

297   **lamellae.** The total duration of the batch job was 47 minutes, plus 12 minutes required for the initial

298   (manual) selection of sample locations by the user. Here, each lamella location is displayed in a single

299   row (marked a, b, c, d, e) and white arrowheads indicate the position of the finished lamella. The cross-

300   shaped fiducial marker acts as scale-bar, with dimensions of 6×6 μm. Columns from left to right show:

301   (i) the fiducial marker is created; (ii) trenches opened with high ion beam current; (iii) further thinning

302   with an intermediate ion beam current and (iv) the completed lamella after final polishing with low

303   ion beam current. Ion beam milling currents for these stages were 2.4 nA, 75 pA, and 26 pA,

304   respectively. The milling procedure runs per column, therefore, each FIB milling stage is completed

305   for every lamella location before proceeding to the next milling stage.

306
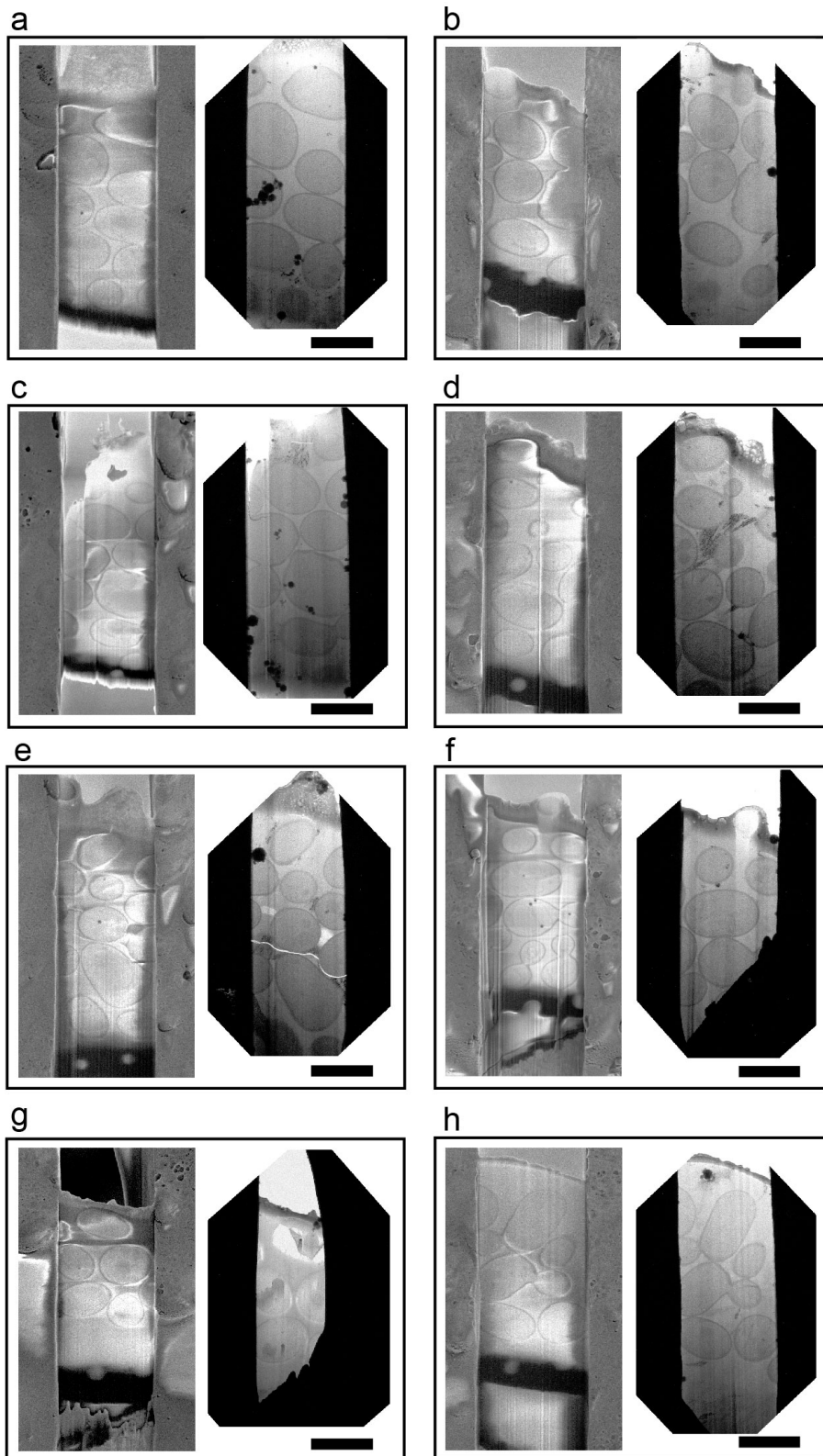
307

Supplementary figure 2: Gallery of 8 lamellae prepared using the procedure described in this article, illustrating quality and pitfalls. Each panel shows on the left a low voltage cryo-SEM image of the lamella surface at the end of the preparation procedure. On the right within each panel there is a low mag cryo-TEM micrograph for each lamella. The images show that the quality is comparable to current preparation approaches. In this gallery, we show potential pitfalls of batch preparation which can be

16

313   easily resolved if the user is aware and careful. The level of curtaining changes in response to lamella

314   length and surface contamination, if the sample thickness is variable the user should select more

315   generous depth for the polishing step to ensure the surface finish is optimal. (a, b) show proper depth

316   selection, while (c–h) show different behaviours when under-polishing). Panels (f) and (g) show that

317   the size of the trenches was not appropriate for the sample thickness, as visible from the cryo-TEM

318   images part of those lamellae is not electron transparent, indicating that there is bulk material

319   underneath the lamella (also visible from the cryo-SEM). Scale-bars are 5 μm.

320

Select Anaconda Prompt - autolamella config.yml

```
(base) C:\Users\genevieb>conda activate fibsem

(fibsem) C:\Users\genevieb>autolamella config.yml
Create a new EMPTY directory to store your output images.
Client connecting to [localhost:7520]...
Client connected to [localhost:7520]
2019-09-17 15:52:57,754 INFO demo_mode: 1.0
fiducial:
  fiducial_image_size_x: 1.5e-06
  fiducial_image_size_y: 1.5e-06
  fiducial_length: 5.0e-07
  fiducial_milling_current: 3.0e-10
  fiducial_milling_depth: 1.0e-07
  fiducial_width: 1.0e-07
  min_distance_from_lamella: 1.0e-07
  reduced_area_resolution: 3072x2048
imaging:
  autocontrast: 0.0
  dwell_time: 1.0e-07
  full_field_ib_images: 1.0
  horizontal_field_width: 5.0e-05
  resolution: 1536x1024
lamella:
  lamella_height: 1.0e-07
  lamella_width: 5.0e-07
  milling_current: 3.0e-10
  milling_depth: 1.0e-06
  overtilt_degrees: 0.0
  protocol_stages:
  - milling_current: 3.0e-10
    milling_depth: 5.0e-07
    percentage_from_lamella_surface: 0.5
    percentage_roi_height: 0.5
  - milling_current: 3.0e-10
    percentage_from_lamella_surface: 0.2
    percentage_roi_height: 0.3
  - milling_current: 3.0e-10
    overtilt_degrees: 2.0
    percentage_from_lamella_surface: 0.0
    percentage_roi_height: 0.2
  total_cut_height: 5.0e-07
save_directory: C:/Users/genevieb/Documents/test/output_directory
system:
  application_file_cleaning_cross_section: Si
  application_file_rectangle: Si
  ip_address: localhost
```

321

322 **Supplementary figure 3: Screenshot of the terminal as the user launches the 'autolamella' program.**

323 The first section of the output consists of a summary of the parameters provided in the configuration

324 file, here named config.yml. The idea is to provide immediate feedback that the file and the

325 parameters selected are the correct ones. This screenshot demonstration has been produced using

326 the Autoscript simulation mode.

327
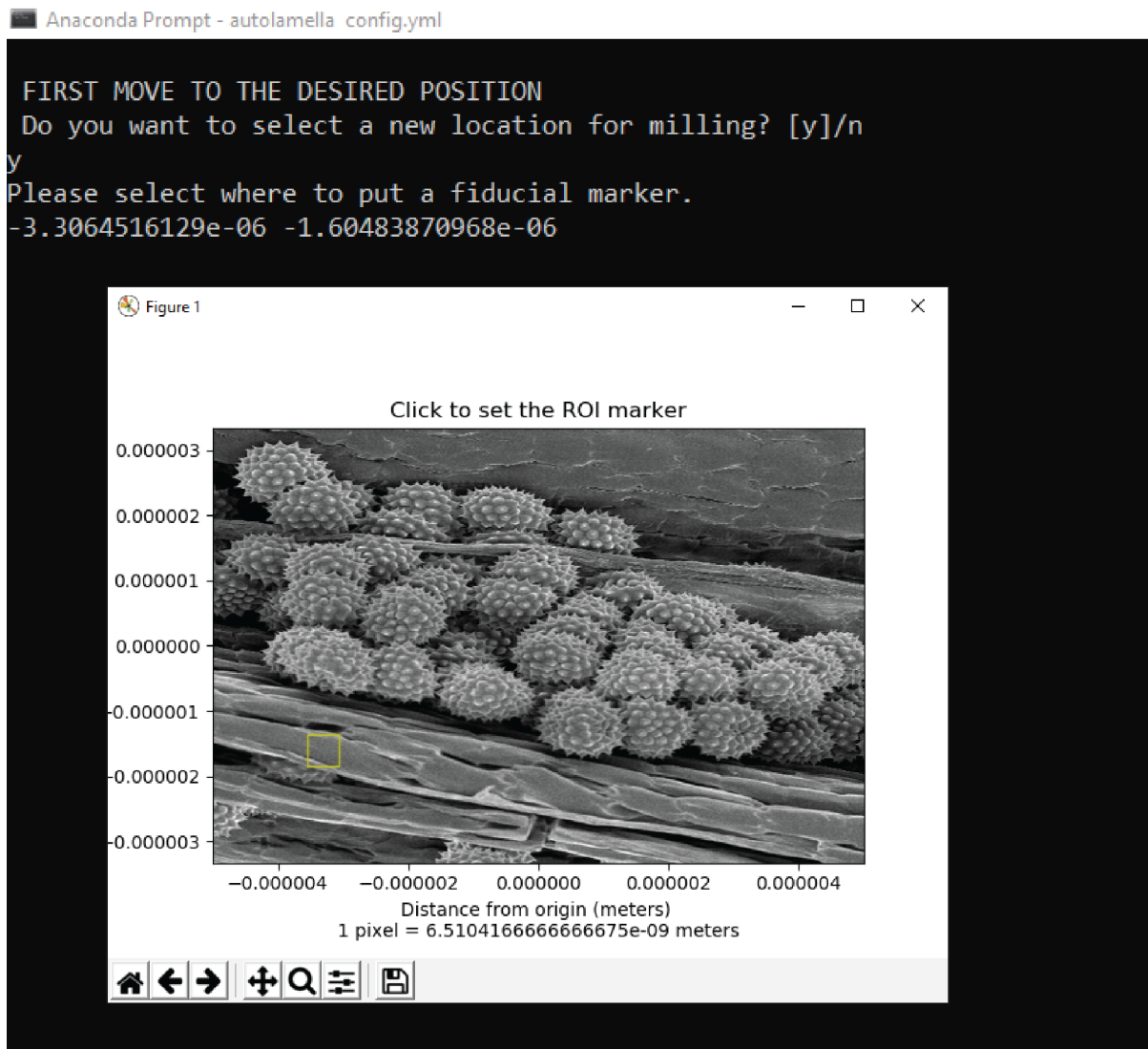
328

329 **Supplementary figure 4: Screenshot of the interactive selection of the tracking area position.** The

330 user finds a suitable location for a lamella interactively using the ThermoFisher Xt UI™. Once the new

331 location has been identified, the user replies yes to the question in the command prompt, "Do you

332 want to select a new location for milling?". The current ion beam image is then displayed in a pop-up

333 window, and the user clicks to select the position for the fiducial marker. The fiducial marker position

334 is indicated with a yellow box, and this position can be adjusted before closing the pop-up window.

335 Closing the window leads to continuing the process. Screenshots have been produced using Autoscript

336 simulation mode.

19

337
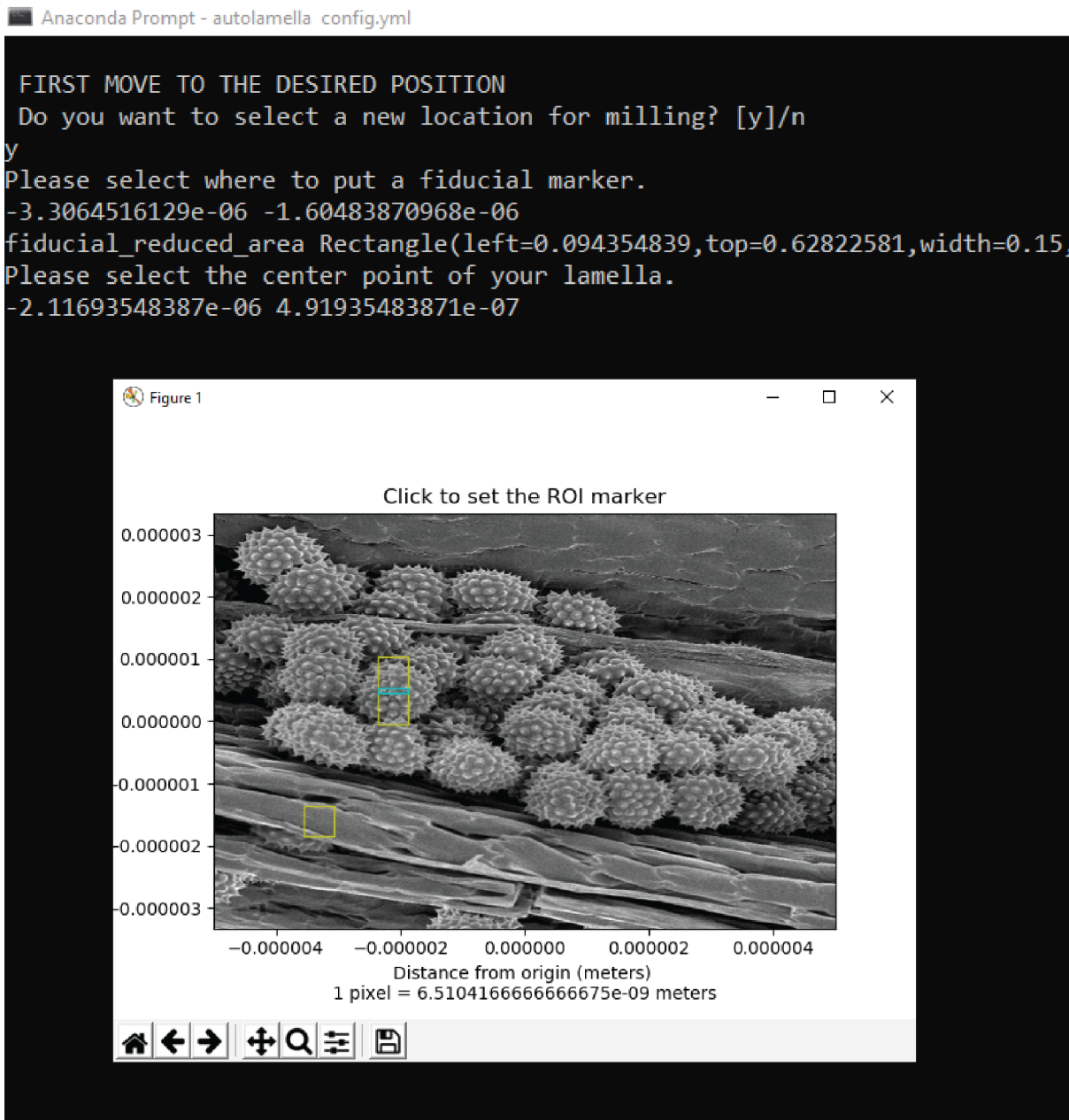
338

339 **Supplementary figure 5: Screenshot of the interactive selection of the lamella position.** The
340 command-line prompt asks the user to "Please select the centre point of your lamella" and a new pop
341 up window displays the current ion beam image with the fiducial marker position shown for reference.
342 The user clicks on the image to choose the position for the lamella. The cyan rectangle indicates the
343 position of the final lamella, and the surrounding yellow box indicates the total size of the trenches as
344 defined in the configuration file. The user can click on in multiple locations to optimise the position of
345 the lamella, and the last coordinates chosen before closing the window will be used for milling.
346 Screenshots have been produced using Autoscript simulation mode.

347

20

```
 Anaconda Prompt

 FIRST MOVE TO THE DESIRED POSITION
 Do you want to select a new location for milling? [y]/n
y
Please select where to put a fiducial marker.
-3.3064516129e-06 -1.60483870968e-06
fiducial_reduced_area Rectangle(left=0.094354839,top=0.62822581,width=0.15,height=0.225)
Please select the center point of your lamella.
-2.11693548387e-06 4.91935483871e-07
Do you want to mill a fiducial marker here? [y]/n
y
Milling fiducial marker...
Do you want to re-mill the fiducial marker? y/[n]
n
If you want a custom milling depth for the LAMELLA enter it here in meters, else- slam on ENTER:


 FIRST MOVE TO THE DESIRED POSITION
 Do you want to select a new location for milling? [y]/n
y
Please select where to put a fiducial marker.
3.70967741935e-06 8.75e-07
fiducial_reduced_area Rectangle(left=0.79596774,top=0.25625,width=0.15,height=0.225)
Please select the center point of your lamella.
1.49193548387e-06 -4.5564516129e-07
Do you want to mill a fiducial marker here? [y]/n
y
Milling fiducial marker...
Do you want to re-mill the fiducial marker? y/[n]
n
If you want a custom milling depth for the LAMELLA enter it here in meters, else- slam on ENTER:


 FIRST MOVE TO THE DESIRED POSITION
 Do you want to select a new location for milling? [y]/n
n
Do you want to mill all samples? yes/no
yes
2019-09-17 16:05:49,659 INFO Protocol stage 1 of 3
2019-09-17 16:05:49,659 INFO Lamella number 1 of 2
2019-09-17 16:05:53,985 INFO Lamella number 2 of 2
2019-09-17 16:05:58,831 INFO Protocol stage 2 of 3
2019-09-17 16:05:58,832 INFO Lamella number 1 of 2
2019-09-17 16:06:03,225 INFO Lamella number 2 of 2
2019-09-17 16:06:09,637 INFO Protocol stage 3 of 3
2019-09-17 16:06:09,638 INFO Lamella number 1 of 2
2019-09-17 16:06:15,716 INFO Lamella number 2 of 2
Finished!
```

Supplementary figure 6: Example output from the command prompt for an automated batch job when preparing two lamellae. After the fiducial mark has been prepared the program images it and provides the option to mill further in case the depth selected does not provide suitable contrast on one particular area. Further the lamella depth can be tuned for each position in case the sample has significant variations. the value should be in meters (e.g. 1e-6 for 1 µm), if the depth specified in the configuration file is acceptable the user should not enter any value. If no more locations are selected (negative answer at the question "Do you want to select a new location for milling?)" the interactive section ends at the question "Do you want to mil all samples?". This screenshot demonstration has been produced using the Autoscript simulation mode.

21

358 **Supplementary video 1: slice by slice video of the tomogram shown in figure 4.**

359

360

361 # References

362 Al-Amoudi, A., Chang, J.-J., Leforestier, A., McDowall, A., Salamin, L. M., Norlén, L. P. O., . . .
363   Dubochet, J. (2004). Cryo-electron microscopy of vitreous sections. *The EMBO Journal,*
364   *23*(18), 3583-3588. doi:10.1038/sj.emboj.7600366

365 Al-Amoudi, A., Studer, D., & Dubochet, J. (2005). Cutting artefacts and cutting process in vitreous
366   sections for cryo-electron microscopy. *Journal of Structural Biology, 150*(1), 109-121.
367   doi:10.1016/j.jsb.2005.01.003

368 Arnold, J., Mahamid, J., Lucic, V., de Marco, A., Fernandez, J.-J., Laugks, T., . . . Plitzko, Jürgen M.
369   (2016). Site-Specific Cryo-focused Ion Beam Sample Preparation Guided by 3D Correlative
370   Microscopy. *Biophysical Journal, 110*(4), 860-869. doi:10.1016/j.bpj.2015.10.053

371 Beck, M., & Baumeister, W. (2016). Cryo-Electron Tomography: Can it Reveal the Molecular
372   Sociology of Cells in Atomic Detail? *Trends in Cell Biology, 26*(11), 825-837.
373   doi:10.1016/j.tcb.2016.08.006

374 Carlson, L. A., de Marco, A., Oberwinkler, H., Habermann, A., Briggs, J. A., Krausslich, H. G., &
375   Grunewald, K. (2010). Cryo electron tomography of native HIV-1 budding sites. *PLoS Pathog,*
376   *6*(11), e1001173. doi:10.1371/journal.ppat.1001173

377 Chreifi, G., Chen, S., Metskas, L. A., Kaplan, M., & Jensen, G. J. (2019). Rapid tilt-series acquisition for
378   electron cryotomography. *Journal of Structural Biology, 205*(2), 163-169.
379   doi:10.1016/j.jsb.2018.12.008

380 Danev, R., Yanagisawa, H., & Kikkawa, M. (2019). Cryo-Electron Microscopy Methodology: Current
381   Aspects and Future Directions. *Trends in Biochemical Sciences*.
382   doi:10.1016/j.tibs.2019.04.008

383 Dubochet, J., Adrian, M., Chang, J.-J., Homo, J.-C., Lepault, J., McDowall, A. W., & Schultz, P. (1988).
384   Cryo-electron microscopy of vitrified specimens. *Quarterly Reviews of Biophysics, 21*(2), 129-
385   228. doi:10.1017/S0033583500004297

386 Eisenstein, F., Danev, R., & Pilhofer, M. (2019). Improved applicability and robustness of fast cryo-
387   electron tomography data acquisition. *Journal of Structural Biology*.
388   doi:10.1016/j.jsb.2019.08.006

389 Gorelick, S., Buckley, G., Gervinskas, G., Johnson, T. K., Handley, A., Caggiano, M. P., . . . de Marco, A.
390   (2019). PIE-scope, integrated cryo-correlative light and FIB/SEM microscopy. *Elife, 8*.
391   doi:10.7554/eLife.45919

392 Hagen, W. J. H., Wan, W., & Briggs, J. A. G. (2017). Implementation of a cryo-electron tomography
393   tilt-scheme optimized for high resolution subtomogram averaging. *Journal of Structural
394   Biology, 197*(2), 191-198. doi:10.1016/j.jsb.2016.06.007

395 Holtz, M. E., Yu, Y., Gao, J., Abruña, H. D., & Muller, D. A. (2013). In Situ Electron Energy-Loss
396   Spectroscopy in Liquids. *Microscopy and Microanalysis, 19*(4), 1027-1035.
397   doi:10.1017/S1431927613001505

398 Hsieh, C., Schmelzer, T., Kishchenko, G., Wagenknecht, T., & Marko, M. (2014). Practical workflow
399   for cryo focused-ion-beam milling of tissues and cells for cryo-TEM tomography. *Journal of
400   Structural Biology, 185*(1), 32-41. doi:10.1016/j.jsb.2013.10.019

401 Hunter, J. D. (2007). Matplotlib: A 2D Graphics Environment. *Computing in Science Engineering, 9*(3),
402   90-95. doi:10.1109/MCSE.2007.55

403 Koning, R. I., Koster, A. J., & Sharp, T. H. (2018). Advances in cryo-electron tomography for biology
404   and medicine. *Annals of Anatomy - Anatomischer Anzeiger, 217*, 82-96.
405   doi:10.1016/j.aanat.2018.02.004

406 Marko, M., Hsieh, C., Schalek, R., Frank, J., & Mannella, C. (2007). Focused-ion-beam thinning of
407   frozen-hydrated biological specimens for cryo-electron microscopy. *Nature Methods, 4*(3),
408   215-217. doi:10.1038/nmeth1014
409 Mastronarde, D. N. (1997). Dual-Axis Tomography: An Approach with Alignment Methods That
410   Preserve Resolution. *Journal of Structural Biology, 120*(3), 343-352.
411   doi:10.1006/jsbi.1997.3919
412 Medeiros, J. M., Böck, D., Weiss, G. L., Kooger, R., Wepf, R. A., & Pilhofer, M. (2018). Robust
413   workflow and instrumentation for cryo-focused ion beam milling of samples for electron
414   cryotomography. *Ultramicroscopy, 190*, 1-11. doi:10.1016/j.ultramic.2018.04.002
415 Oliphant, T. E. (2007). Python for Scientific Computing. *Computing in Science & Engineering, 9*(3), 10-
416   20. doi:10.1109/MCSE.2007.58
417 Pettersen, E. F., Goddard, T. D., Huang, C. C., Couch, G. S., Greenblatt, D. M., Meng, E. C., & Ferrin, T.
418   E. (2004). UCSF Chimera--a visualization system for exploratory research and analysis. *J
419   Comput Chem, 25*(13), 1605-1612. doi:10.1002/jcc.20084
420 Rigort, A., Bäuerlein, F. J. B., Villa, E., Eibauer, M., Laugks, T., Baumeister, W., & Plitzko, J. M. (2012).
421   Focused ion beam micromachining of eukaryotic cells for cryoelectron tomography.
422   *Proceedings of the National Academy of Sciences, 109*(12), 4449-4454.
423   doi:10.1073/pnas.1201333109
424 Schaffer, M., Engel, B. D., Laugks, T., Mahamid, J., Plitzko, J. M., & Baumeister, W. (2015). Cryo-
425   focused Ion Beam Sample Preparation for Imaging Vitreous Cells by Cryo-electron
426   Tomography. *Bio-protocol, 5*(17).
427 Schaffer, M., Mahamid, J., Engel, B. D., Laugks, T., Baumeister, W., & Plitzko, J. M. (2017). Optimized
428   cryo-focused ion beam sample preparation aimed at in situ structural studies of membrane
429   proteins. *Journal of Structural Biology, 197*(2), 73-82. doi:10.1016/j.jsb.2016.07.010
430 Schindelin, J., Arganda-Carreras, I., Frise, E., Kaynig, V., Longair, M., Pietzsch, T., . . . Cardona, A.
431   (2012). Fiji: an open-source platform for biological-image analysis. *Nat Methods, 9*(7), 676-
432   682. doi:10.1038/nmeth.2019
433 Stauffer, S., Rahman, S. A., de Marco, A., Carlson, L. A., Glass, B., Oberwinkler, H., . . . Krausslich, H.
434   G. (2014). The nucleocapsid domain of Gag is dispensable for actin incorporation into HIV-1
435   and for association of viral budding sites with cortical F-actin. *J Virol, 88*(14), 7893-7903.
436   doi:10.1128/JVI.00428-14
437 van der Walt, S., Colbert, S. C., & Varoquaux, G. (2011). The NumPy Array: A Structure for Efficient
438   Numerical Computation. *Computing in Science Engineering, 13*(2), 22-30.
439   doi:10.1109/MCSE.2011.37
440 van der Walt, S., Schönberger, J. L., Nunez-Iglesias, J., Boulogne, F., Warner, J. D., Yager, N., . . . Yu, T.
441   (2014). scikit-image: image processing in Python. *PeerJ, 2*, e453. doi:10.7717/peerj.453
442 Villa, E., Schaffer, M., Plitzko, J. M., & Baumeister, W. (2013). Opening windows into the cell:
443   focused-ion-beam milling for cryo-electron tomography. *Current Opinion in Structural
444   Biology, 23*(5), 771-777. doi:10.1016/j.sbi.2013.08.006
445 Weber, M. S., Wojtynek, M., & Medalia, O. (2019). Cellular and Structural Studies of Eukaryotic Cells
446   by Cryo-Electron Tomography. *Cells, 8*(1). doi:10.3390/cells8010057
447 Wolff, G., Limpens, R. W. A. L., Zheng, S., Snijder, E. J., Agard, D. A., Koster, A. J., & Bárcena, M.
448   (2019). Mind the gap: micro-expansion joints drastically decrease the bending of FIB-milled
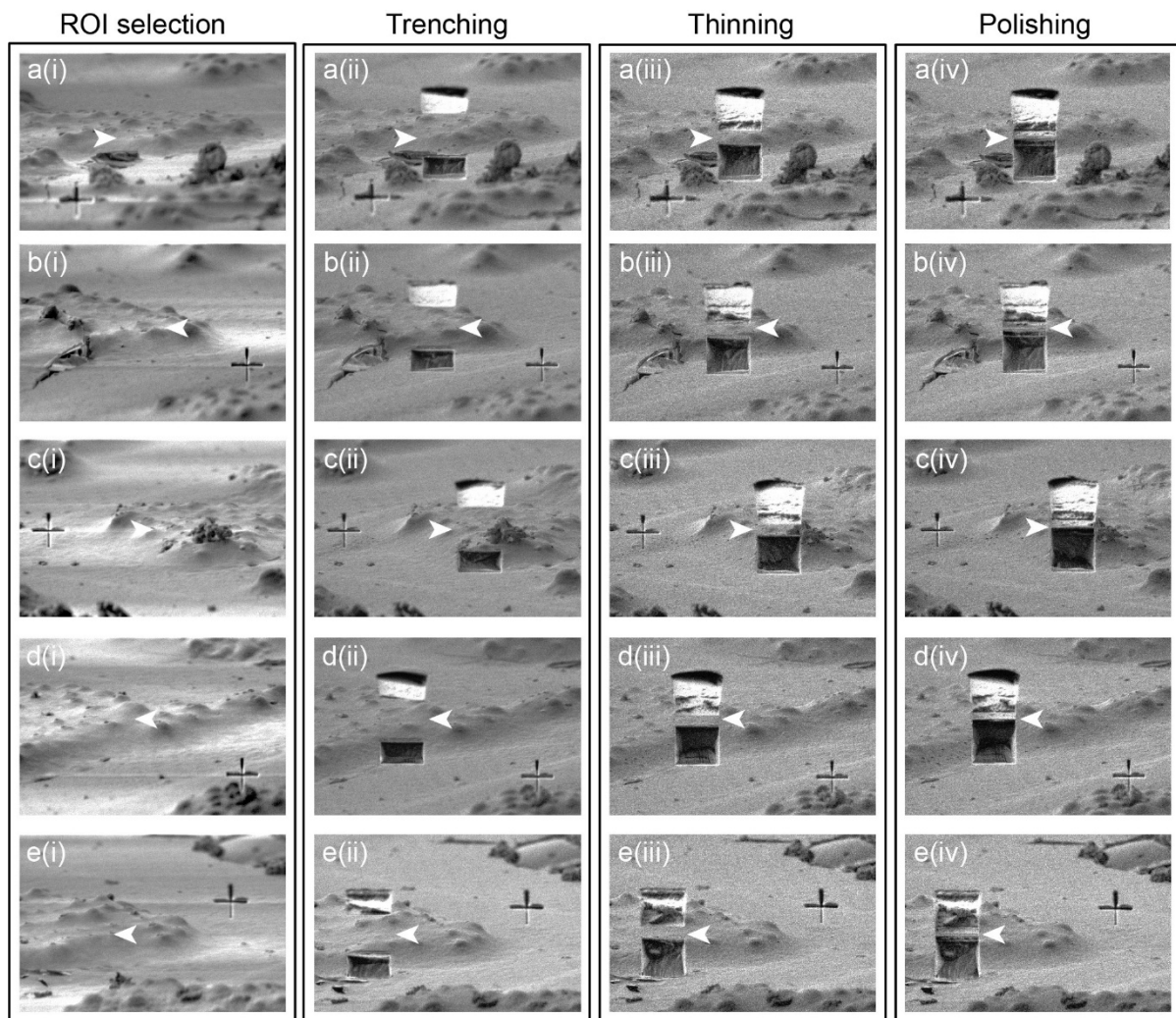449   cryo-lamellae. *bioRxiv*, 656447. doi:10.1101/656447

450

Supplementary Information

Automated cryo-lamella preparation for high-throughput *in-situ* structural biology

Authors:

Genevieve Buckley, Gediminas Gervinskas, Cyntia Taveneau, Hari Venugopal, James C. Whisstock, Alex de Marco

Supplementary figure 1: Ion beam images acquired throughout a single batch job consisting of 5 lamellae. The total duration of the batch job was 47 minutes, plus 12 minutes required for the initial (manual) selection of sample locations by the user. Here, each lamella location is displayed in a single row (marked a, b, c, d, e) and white arrowheads indicate the position of the finished lamella. The cross-shaped fiducial marker acts as scale-bar, with dimensions of 6×6 μm. Columns from left to right show: (i) the fiducial marker is created; (ii) trenches opened with high ion beam current; (iii) further thinning

with an intermediate ion beam current and (iv) the completed lamella after final polishing with low ion beam current. Ion beam milling currents for these stages were 2.4 nA, 75 pA, and 26 pA, respectively. The milling procedure runs per column, therefore, each FIB milling stage is completed for every lamella location before proceeding to the next milling stage.
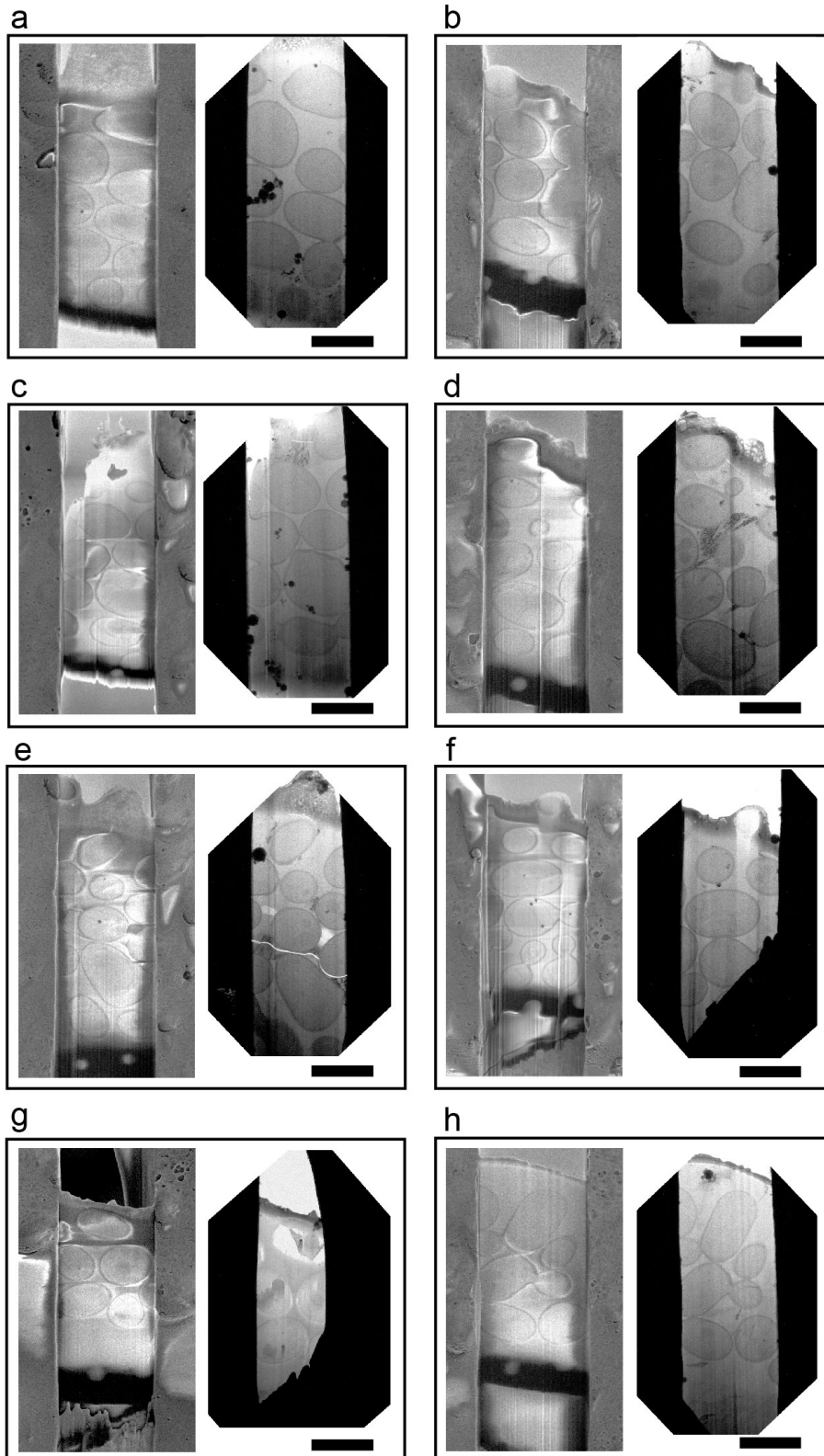
Supplementary figure 2: Gallery of 8 lamellae prepared using the procedure described in this article, illustrating quality and pitfalls. Each panel shows on the left a low voltage cryo-SEM image of the lamella surface at the end of the preparation procedure. On the right within each panel there is a low mag cryo-TEM micrograph for each lamella. The images show that the quality is comparable to current preparation approaches. In this gallery, we show potential pitfalls of batch preparation which can be easily resolved if the user is aware and careful. The level of curtaining changes in response to lamella length and surface contamination, if the sample thickness is variable the user should select more generous depth for the polishing step to ensure the surface finish is optimal. (a, b) show proper depth selection, while (c–h) show different behaviours when under-polishing). Panels (f) and (g) show that the size of the trenches was not appropriate for the sample thickness, as visible from the cryo-TEM images part of those lamellae is not electron transparent, indicating that there is bulk material underneath the lamella (also visible from the cryo-SEM). Scale-bars are 5 μm.

▨ Select Anaconda Prompt - autolamella config.yml

```
(base) C:\Users\genevieb>conda activate fibsem

(fibsem) C:\Users\genevieb>autolamella config.yml
Create a new EMPTY directory to store your output images.
Client connecting to [localhost:7520]...
Client connected to [localhost:7520]
2019-09-17 15:52:57,754 INFO demo_mode: 1.0
fiducial:
  fiducial_image_size_x: 1.5e-06
  fiducial_image_size_y: 1.5e-06
  fiducial_length: 5.0e-07
  fiducial_milling_current: 3.0e-10
  fiducial_milling_depth: 1.0e-07
  fiducial_width: 1.0e-07
  min_distance_from_lamella: 1.0e-07
  reduced_area_resolution: 3072x2048
imaging:
  autocontrast: 0.0
  dwell_time: 1.0e-07
  full_field_ib_images: 1.0
  horizontal_field_width: 5.0e-05
  resolution: 1536x1024
lamella:
  lamella_height: 1.0e-07
  lamella_width: 5.0e-07
  milling_current: 3.0e-10
  milling_depth: 1.0e-06
  overtilt_degrees: 0.0
  protocol_stages:
  - milling_current: 3.0e-10
    milling_depth: 5.0e-07
    percentage_from_lamella_surface: 0.5
    percentage_roi_height: 0.5
  - milling_current: 3.0e-10
    percentage_from_lamella_surface: 0.2
    percentage_roi_height: 0.3
  - milling_current: 3.0e-10
    overtilt_degrees: 2.0
    percentage_from_lamella_surface: 0.0
    percentage_roi_height: 0.2
  total_cut_height: 5.0e-07
save_directory: C:/Users/genevieb/Documents/test/output_directory
system:
  application_file_cleaning_cross_section: Si
  application_file_rectangle: Si
  ip_address: localhost
```

Supplementary figure 3: Screenshot of the terminal as the user launches the 'autolamella' program.
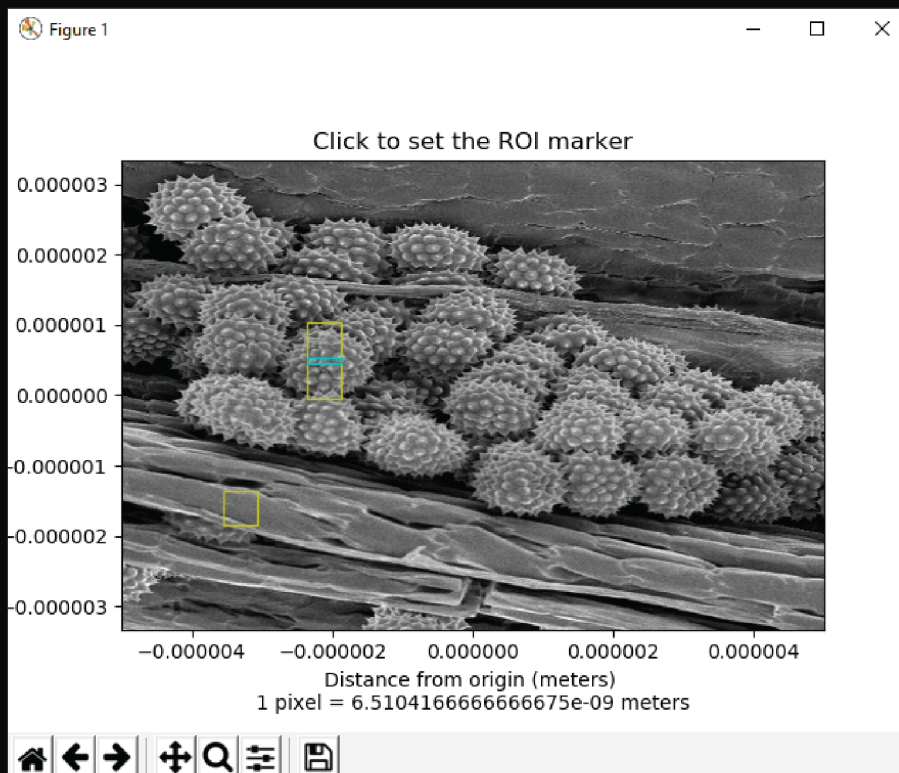The first section of the output consists of a summary of the parameters provided in the configuration file, here named config.yml. The idea is to provide immediate feedback that the file and the parameters selected are the correct ones. This screenshot demonstration has been produced using the Autoscript simulation mode.
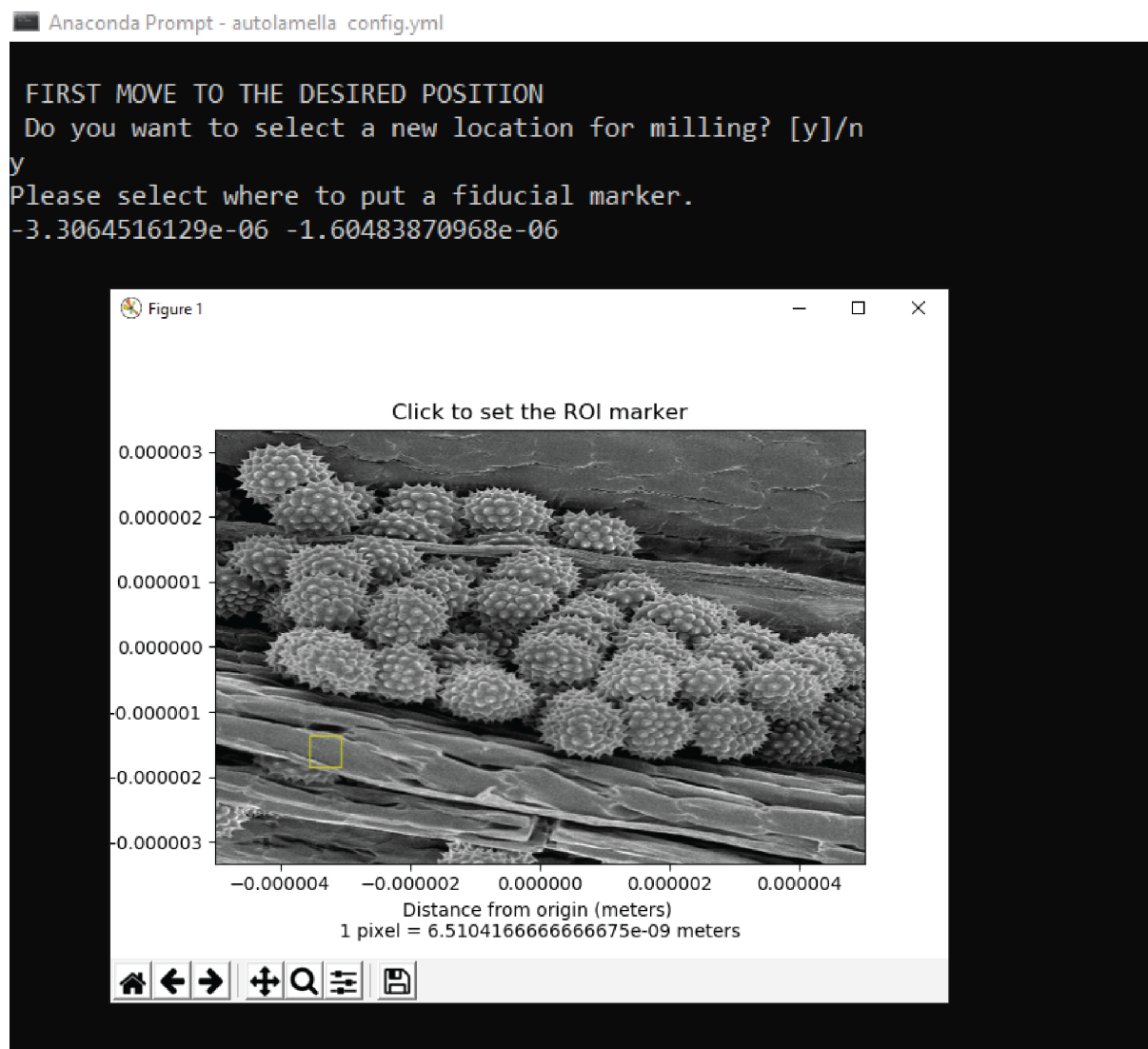
Supplementary figure 4: Screenshot of the interactive selection of the tracking area position. The user finds a suitable location for a lamella interactively using the ThermoFisher Xt UI™. Once the new location has been identified, the user replies yes to the question in the command prompt, "Do you want to select a new location for milling?". The current ion beam image is then displayed in a pop-up window, and the user clicks to select the position for the fiducial marker. The fiducial marker position is indicated with a yellow box, and this position can be adjusted before closing the pop-up window. Closing the window leads to continuing the process. Screenshots have been produced using Autoscript simulation mode.

Supplementary figure 5: Screenshot of the interactive selection of the lamella position. The command-line prompt asks the user to "Please select the centre point of your lamella" and a new pop up window displays the current ion beam image with the fiducial marker position shown for reference. The user clicks on the image to choose the position for the lamella. The cyan rectangle indicates the position of the final lamella, and the surrounding yellow box indicates the total size of the trenches as defined in the configuration file. The user can click on in multiple locations to optimise the position of the lamella, and the last coordinates chosen before closing the window will be used for milling. Screenshots have been produced using Autoscript simulation mode.

```
■ Anaconda Prompt

 FIRST MOVE TO THE DESIRED POSITION
 Do you want to select a new location for milling? [y]/n
y
Please select where to put a fiducial marker.
-3.3064516129e-06 -1.60483870968e-06
fiducial_reduced_area Rectangle(left=0.094354839,top=0.62822581,width=0.15,height=0.225)
Please select the center point of your lamella.
-2.11693548387e-06 4.91935483871e-07
Do you want to mill a fiducial marker here? [y]/n
y
Milling fiducial marker...
Do you want to re-mill the fiducial marker? y/[n]
n
If you want a custom milling depth for the LAMELLA enter it here in meters, else- slam on ENTER:


 FIRST MOVE TO THE DESIRED POSITION
 Do you want to select a new location for milling? [y]/n
y
Please select where to put a fiducial marker.
3.70967741935e-06 8.75e-07
fiducial_reduced_area Rectangle(left=0.79596774,top=0.25625,width=0.15,height=0.225)
Please select the center point of your lamella.
1.49193548387e-06 -4.5564516129e-07
Do you want to mill a fiducial marker here? [y]/n
y
Milling fiducial marker...
Do you want to re-mill the fiducial marker? y/[n]
n
If you want a custom milling depth for the LAMELLA enter it here in meters, else- slam on ENTER:


 FIRST MOVE TO THE DESIRED POSITION
 Do you want to select a new location for milling? [y]/n
n
Do you want to mill all samples? yes/no
yes
2019-09-17 16:05:49,659 INFO Protocol stage 1 of 3
2019-09-17 16:05:49,659 INFO Lamella number 1 of 2
2019-09-17 16:05:53,985 INFO Lamella number 2 of 2
2019-09-17 16:05:58,831 INFO Protocol stage 2 of 3
2019-09-17 16:05:58,832 INFO Lamella number 1 of 2
2019-09-17 16:06:03,225 INFO Lamella number 2 of 2
2019-09-17 16:06:09,637 INFO Protocol stage 3 of 3
2019-09-17 16:06:09,638 INFO Lamella number 1 of 2
2019-09-17 16:06:15,716 INFO Lamella number 2 of 2
Finished!
```

Supplementary figure 6: Example output from the command prompt for an automated batch job when preparing two lamellae. After the fiducial mark has been prepared the program images it and provides the option to mill further in case the depth selected does not provide suitable contrast on one particular area. Further the lamella depth can be tuned for each position in case the sample has significant variations. the value should be in meters (e.g. 1e-6 for 1 μm), if the depth specified in the configuration file is acceptable the user should not enter any value. If no more locations are selected (negative answer at the question "Do you want to select a new location for milling?)" the interactive section ends at the question "Do you want to mil all samples?". This screenshot demonstration has been produced using the Autoscript simulation mode.

Supplementary video 1: slice by slice video of the tomogram shown in figure 4.

Supplementary video 1: slice by slice video of the tomogram shown in figure 4.